A probabilistic approach for the estimation of angle kappa in infants

Dmitri Model
University of Toronto
dmitry.model@gmail.com

Moshe Eizenman
University of Toronto
eizenm@ecf.utornot.ca

Abstract

This paper presents a probabilistic approach for the estimation of the angle between the optical and visual axes (angle kappa) in infants. The approach assumes that when patterned calibration targets are presented on a uniform background, subjects are more likely to look at the calibration targets than at the uniform background, but it does not require accurate and continuous fixation on presented targets. Simulations results show that when subjects attend to roughly half of the presented targets, angle kappa can be estimated accurately with low probability (< 1%) of false detection. In experiments with five babies who attended to the calibration target for only 47% of the time (range from 26% to 70%), the average difference between repeated measurements of angle kappa was 0.04 ± 0.31°.

Keywords: *Eye Tracking, Remote Gaze Estimation, Calibration-Free, Infants, Uncooperative Subjects.*

1 Introduction

State-of-the-art Remote Eye Gaze Tracking (REGT) systems that use a stereo pair of video cameras can estimate the center of curvature of the cornea, **c**, and the *optical* axis of the eye, **ω**, without any user calibration [Guestrin and Eizemnan 2007; Shih and Liu 2004]. However, since human gaze is not directed along the *optical* axis, but rather along the *visual* axis, a subject-dependant angle between the optical and visual axes (angle kappa) should be estimated. In cooperative subjects, a one-point calibration procedure can be used to estimate angle kappa. During this calibration procedure, the subject is required to look at a single calibration target, and it is assumed that the visual axis intersects with the center of the target. However, in studies with uncooperative subjects (e.g., young children or mentally challenged people), even such a simple procedure cannot be performed reliably.

Several "user-calibration-free" approaches for remote gaze estimation have been suggested in the literature. Shih et al assumed that the visual and optical axis coincide (angle kappa is zero) [Shih et al. 2000], while Nagamatsu et al used a midpoint of intersection of the optical axes of both eyes as approximation for the Point-of-Gaze (PoG) [Nagamatsu et al. 2010]. However, such approaches result in significant subject-dependent gaze-estimation errors [Model and Eizenman 2010a]. Model and Eizenman suggested an automated method for the estimation of angle kappa [Model and Eizenman 2010a; Model and Eizenman 2010b]. However for accurate results, such method requires either a very accurate REGT system (RMS error in the estimation of the optical axis < 0.1°) or observation surface that consists of multiple planes (please see [Model and Eizenman 2010a; Model and Eizenman 2010b] for details), which limits the practical utility of such approach.

This space should be left empty

This paper presents an automatic calibration procedure that is designed for infants. It is based on inherent tendency of babies to look at patterned stimuli presented on a uniform background [Fantz et al. 1975]. Therefore, if several stimuli (animated images) are presented at different locations on a uniform background, there is a higher likelihood that infants will look at the presented stimuli than at any other point. The probabilistic approach to the estimation of angle Kappa is based on this observation. During the presentation of the visual stimuli the suggested Model-Eizenman algorithm (M-E algorithm, hereafter) continuously estimates the angle between the optical and visual axes under the assumption that the infant fixates the presented point (see Section 2.1). At the end of the presentation, the resulting estimates of angle Kappa form a distribution from which a determination of the true angle Kappa can be obtained. If there is no correlation between the infant's gaze and the positions of the visual stimuli, the distribution of the measured angles will tend to be uniform. On the other hand, if the infant did look at the presented targets from time to time, there will be a dominant peak in the distribution of the measured angles that corresponds to an angle between the optical and visual axes. Therefore, the M-E algorithm consists of two stages: Estimation and Validation. The M-E algorithm is described in details in Section 2.2. Since the M-E procedure is probabilistic in nature, the confidence measure in the outcome of M-E is derived in Section 2.3. Experimental results with five infants are presented in Section 3. Finally, discussion and conclusions are presented in Section 4.

2 Method

In the following analysis, all points are represented as 3-D column vectors (bold font) in a right-handed Cartesian World-fixed Coordinate System (WCS).

Figure 1 presents a simplified schematic diagram of the eye [Model and Eizenman 2010a]. The line connecting the center of curvature of the cornea with the center of the pupil defines the *optical* axis. The line connecting the center of the fovea with the center of curvature of the cornea defines the *visual* axis or the line-of-gaze. The average magnitude of the angle between the *optical* and *visual* axes is 5°. This angle has both horizontal

(nasal) and vertical components, which exhibit considerable inter-personal variation [Carpenter 1977].

Two coordinate systems are used in this paper. The first coordinate system is a stationary right-handed Cartesian World Coordinate System (WCS) with the origin at the center of the main display, the X_w-axis in the horizontal direction, the Y_w-axis in the vertical direction and the Z_w-axis perpendicular to the display (see Figure 1). This coordinate system is used to define PoG relative to fixed objects in space (e.g., computer monitor).

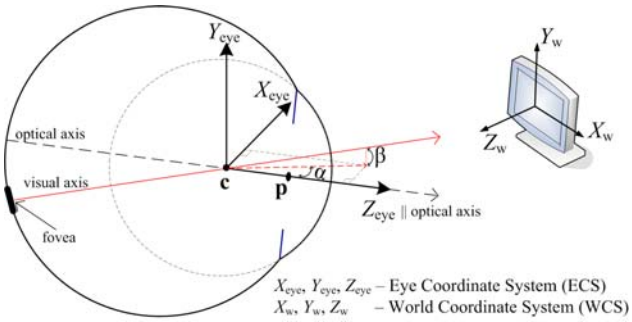

Figure 1. *A simplified schematic diagram of the eye (not to scale). The optical axis,* **ω** *(the axis of symmetry of the eye) passes through the center of curvature of the cornea,* **c***, and the center of the pupil,* **p**. *The visual axis of the eye (the line-of-sight),* **v***, connects the fovea (the region of the highest visual acuity on the retina) with* **c**.

The second coordinate system is a non-stationary right-handed Cartesian Eye Coordinate System (ECS), which is attached to the eye, with the origin at the center of curvature of the cornea, the Z_{eye} axis that coincides with the optical axis of the eye and X_{eye} and Y_{eye} axes that, in the primary gaze position, are in the horizontal and vertical directions, respectively. The X_{eye}-Y_{eye} plane rotates according to Listing's law [Helmholtz 1924] around the Z_{eye} axis for different gaze directions.

In the ECS, the unknown 3D angle between the *optical* and the *visual* axes of the eye can be expressed by the horizontal, α, and vertical, β, components of this angle (see Figure 1). The unit vector in the direction of the *visual* axis with respect to the ECS, $\mathbf{v}_{ECS}$, is then expressed as:

$$\mathbf{v}_{ECS}(\alpha,\beta)=\begin{bmatrix}-\sin(\alpha)\cos(\beta)\\ \sin(\beta)\\ \cos(\alpha)\cos(\beta)\end{bmatrix} \quad (1)$$

The unit vector in the direction of the visual axis with respect to the WCS, $\mathbf{v}$, can be expressed as:

$$\mathbf{v}(\alpha,\beta)=\mathbf{R}\,\mathbf{v}_{ECS}(\alpha,\beta) \quad (2)$$

where $\mathbf{R}=[\mathbf{i}_{ECS}\ \mathbf{j}_{ECS}\ \mathbf{k}_{ECS}]$ is the rotation matrix from the ECS to the WCS and $\mathbf{i}_{ECS}$, $\mathbf{j}_{ECS}$ and $\mathbf{k}_{ECS}$ are the unit vectors in the direction of the X_{eye}, Y_{eye} and Z_{eye} axes with respect to the WCS, respectively. Note that $\mathbf{i}_{ECS}$, $\mathbf{j}_{ECS}$ and $\mathbf{k}_{ECS}$ are independent of α and β and $\mathbf{R}$ can be readily calculated from the orientation of the optical axis of the eye and Listing's law [Guestrin and Eizenman 2010; Helmholtz 1924].

Because the visual axis goes through the center of curvature of the cornea, **c**, the PoG, **g**, in the WCS is given by:

$$\mathbf{g}=\mathbf{c}+\mu\mathbf{v}(\alpha,\beta)=\mathbf{c}+\mu\,\mathbf{R}\,\mathbf{v}_{ECS}(\alpha,\beta) \quad (3)$$

where μ is a line parameter, proportional to the distance from the eye to the monitor.

2.1 Estimation of angle kappa for a single time sample

As was shown in [Guestrin and Eizenman 2008], under the assumption that the subject fixates on a calibration target, the horizontal, α, and vertical, β, components of angle kappa (the angle between the optical and visual axes) can be estimated as follows.

Let's denote, **ж**, the position of the calibration target in 3-D. Then, the unit vector in the direction of the line that connects the center of curvature of the cornea, **c**, and **ж** is given by

$$\mathbf{d}=\frac{\mathbf{ж}-\mathbf{c}}{\|\mathbf{ж}-\mathbf{c}\|}. \quad (4)$$

If one assumes that the target is being looked at, according to (3), the visual axis is, in fact, aligned with **d**:

$$\mathbf{v}(\alpha,\beta)=\mathbf{d}=\frac{\mathbf{ж}-\mathbf{c}}{\|\mathbf{ж}-\mathbf{c}\|}. \quad (5)$$

Using (2), the visual axis in the ECS is given by

$$\mathbf{v}_{ECS}(\alpha,\beta)=\mathbf{R}^{T}\,\mathbf{v}(\alpha,\beta)=\mathbf{R}^{T}\,\frac{\mathbf{ж}-\mathbf{c}}{\|\mathbf{ж}-\mathbf{c}\|}. \quad (6)$$

Since $\mathbf{v}_{ECS}(\alpha,\beta)$ can also be expressed by Eq. (1):

$$\begin{bmatrix}-\sin(\alpha)\cos(\beta)\\ \sin(\beta)\\ \cos(\alpha)\cos(\beta)\end{bmatrix}=\mathbf{R}^{T}\,\frac{\mathbf{ж}-\mathbf{c}}{\|\mathbf{ж}-\mathbf{c}\|}. \quad (7)$$

The angles α and β can be reconstructed directly from (7) as follows

$$\alpha=\arctan\left(-\frac{\left(\mathbf{R}^{T}\frac{\mathbf{ж}-\mathbf{c}}{\|\mathbf{ж}-\mathbf{c}\|}\right)\bullet\hat{\mathbf{x}}}{\left(\mathbf{R}^{T}\frac{\mathbf{ж}-\mathbf{c}}{\|\mathbf{ж}-\mathbf{c}\|}\right)\bullet\hat{\mathbf{z}}}\right) \quad (8)$$

$$\beta=\arcsin\left(\left(\mathbf{R}^{T}\frac{\mathbf{ж}-\mathbf{c}}{\|\mathbf{ж}-\mathbf{c}\|}\right)\bullet\hat{\mathbf{y}}\right) \quad (9)$$

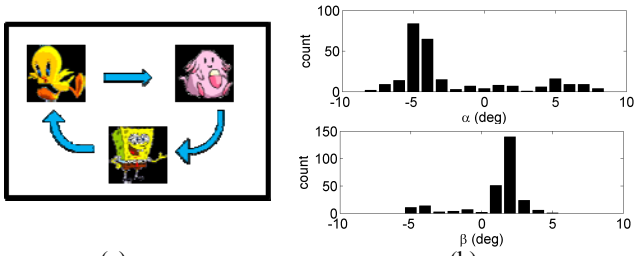

(a) (b)

Figure 2. (a) Example of a sequence of attractive stimuli presented on a computer monitor at different locations (not to scale); (b) Histograms of α and β angles of the right eye measured with an 8 months old infant.

where $\hat{\mathbf{x}}$, $\hat{\mathbf{y}}$ and $\hat{\mathbf{z}}$ are unit vectors in the directions of X_w, Y_w and Z_w respectively, and ' • ' denotes dot product.

2.2 Estimation of angle kappa with uncooperative subjects

As shown in the previous section, the horizontal, α, and vertical, β, components of angle kappa (the angle between the optical and visual axes) can be easily estimated if the subject fixates on a calibration target. With infants, unfortunately, it is impossible to control when and for how long they will look at the calibration target. However, based on the natural tendency of humans to look at visual stimuli with distinctive features [Fantz et al. 1975; Koch and Ullman 1985], one can assume that there is higher likelihood that infants will fixate on the stimulus rather than anywhere else on the computer monitor.

Based on the above assumption, the following strategy can be used to estimate angle kappa. A sequence of visual stimuli is presented at different locations on a computer screen (Figure 2 (a)). The angles α_t, and β_t for each time instant t, are calculated under the assumption that the infant is fixating on the presented stimulus using equations (8) and (9). Then, a histogram of α_t, and β_t, t =1..N is created. Example of such a histogram for a sequence of 9 stimuli (50 estimates/stimuli for a total of N = 450 estimates) that were presented to an 8 months old infant is shown in Figure 2(b).

If the subject fixates exclusively on the presented stimuli, similar values of α_i, and β_i, should be computed for all N measurements (i.e., all α_t or β_t should fall in a single bin of the histogram). If, on the other hand, the subject fixates on points that are uncorrelated with the presented stimuli, the distribution will become more uniform and at the limit the histogram will resemble a uniform distribution. In Figure 2(b), the histograms of α_t and β_t exhibit dominant peaks that correspond to all the time instances for which the infant looked at the stimuli, while points in the histograms that do not belong to these peaks correspond to time instances for which the infant looked elsewhere. In this particular example the infant looked at the stimuli for only 37% of the time that the visual stimuli were presented on the screen. For the five infants who participated in the study, the average percentage of time that infants looked at the stimuli was 47% (range from 26% to 70%).

Estimation of angle kappa in infants is summarized in Algorithm 1.

Algorithm 1
Estimation of angle kappa

1. Present a sequence of visual stimuli with limited spatial extent at pseudo-random locations on a computer monitor.
2. For each time instant t, calculate α_t, and β_t using equations (8) and (9), respectively, under the assumption that the subject is looking at the presented stimuli.
3. Find time instances for inliers in α, $\mathbf{t}_\alpha$:
   i. Partition all $\{\alpha_t \mid -10° < \alpha_t < 10°, t=1..N\}$, (angle kappa is known to be within ±5° for adult subjects [Carpenter 1977; Hashemi et al. 2010] and up to ±8° in infants [Schaeffel 2002]) into bins of width W. Estimates of α_i, outside the range of ±10° are inconsistent with the physiological properties of the human eye and can be discarded).
   ii. Select the bin with the largest count of data points.
   iii. Calculate the average value, $\bar{\alpha}$, of all the data points in the selected bin and two adjacent bins.
   iv. Inliers are α_t-s that satisfy $|\alpha_t - \bar{\alpha}| < W$, i.e., $\mathbf{t}_\alpha = \{t \mid |\alpha_t - \bar{\alpha}| < W\}$
4. Find all the time instances for inliers in β, $\mathbf{t}_\beta$ using the procedure described in Step 3.
5. The time instances for inliers in both α and β are given by: $\mathbf{t}_{in} = \mathbf{t}_\alpha \cap \mathbf{t}_\beta$ and the number of all inliers is N_{in}.
6. The estimated α_t, and β_t are given by

$$\tilde{\alpha} = \frac{1}{N_{in}} \sum_{t \in \mathbf{t}_{in}} \alpha_t \quad (10)$$

$$\tilde{\beta} = \frac{1}{N_{in}} \sum_{t \in \mathbf{t}_{in}} \beta_t \quad (11)$$

respectively.

2.3 Confidence measure for the outcome of the M-E procedure

Algorithm 1 analyzes the distribution of angular offsets between $\boldsymbol{\omega}$ (the optical axis of the eye) and a line $\mathbf{d}$ (a line that connect $\mathbf{c}$ and the center of the target). When the subject looks at the target, line $\mathbf{d}$ is aligned with the visual axis of the eye and the offset is equal to angle Kappa. Algorithm 1 selects an offset ($\tilde{\alpha}$ and $\tilde{\beta}$) that results in the maximum number of inlier samples, N_{in}. In this section we estimate the probability that Algorithm 1 will select/estimate $\tilde{\alpha}$ and $\tilde{\beta}$ from the recorded data points that are not associated with fixations on the presented targets (i.e., the probability of false detection).

In Algorithm 1, the angular offsets, α_t, and β_t, between $\boldsymbol{\omega}_t$ and the target being presented, $\mathbf{d}_k$, are measured for each time instant t=1..N. However, α_t, t=1..N (as well as β_t, t=1..N) are not independent because of temporal correlation between consecutive $\boldsymbol{\omega}_t$ and possible spatial correlation if a subject re-visits the same salient point several times. To remove such correlations, let's define a cluster, $\boldsymbol{\Gamma}$, as a set of α_t, and β_t, that are within ±Φ of the

center of such cluster during the presentation of the k-th target ($t = T_k...(T_{k+1}-1)$, where T_k is the time instant when the k-th target was presented). Under this definition, if the subject fixates the same point during several consecutive time samples or/and revisits the same point several times during the presentation of the k-th target, this will still constitute a single cluster. If Φ is large enough (e.g., equal to the half of the angular extent of the target presented), the positions of the clusters during the presentation of the k-th target can be assumed to be independent. Furthermore, since the positions of the targets are randomized ($\mathbf{d}_k$ k=1..K, are independent random variables), $\mathbf{\Gamma}_m$ m=1..M, are also independent across all targets. Even if a subject keeps fixating the same point on the screen, i.e., $\boldsymbol{\omega}_t$ is constant, the angular offsets between $\boldsymbol{\omega}_t$ and $\mathbf{d}_k$ are not, because $\mathbf{d}_k$ are random and independent of $\boldsymbol{\omega}_t$.

Let's assume that if a subject *does not* pay attention to the stimuli, $\mathbf{\Gamma}_m$ is equally likely to fall anywhere within $\pm\Omega$ around $\mathbf{d}_k$. That is, $\mathbf{\Gamma}_m$, m=1..M, are independent uniformly distributed random variables within $\pm\Omega$. If during the experiment, there were M clusters in total with M_{in} 'inlier' clusters (such clusters that correspond to inlier samples as identified by the Algorithm 1), the probability of such scenario (to have M_{in} overlapping clusters out of M) under the assumption that the subject *does not* pay attention to the stimuli can be estimated using Monte-Carlo simulations. In other words, the purpose of this simulation is to estimate the probability of having M_{in} overlapping clusters, when the subject's gaze is independent of the position of the presented stimuli.

Table 1 Probability of having M_{in} 'inlier' clusters out of M clusters, under the assumption of a uniform distribution of clusters within ±10° of d.

M \ M_{in}	1	2	3	4	5	6	7	8	9
1	1	-	-	-	-	-	-	-	-
2	0.966	0.034	-	-	-	-	-	-	-
3	0.888	0.111	0.001	-	-	-	-	-	-
4	0.802	0.195	0.003	0	-	-	-	-	-
5	0.683	0.311	0.006	0	0	-	-	-	-
6	0.569	0.416	0.014	0	0	0	-	-	-
7	0.444	0.528	0.028	0.001	0	0	0	-	-
8	0.343	0.617	0.039	0.001	0	0	0	0	-
9	0.251	0.695	0.054	0.001	0	0	0	0	0
10	0.175	0.746	0.078	0.002	0	0	0	0	0
11	0.119	0.772	0.105	0.004	0	0	0	0	0
12	0.081	0.787	0.128	0.005	0	0	0	0	0
13	0.043	0.788	0.160	0.008	0	0	0	0	0
14	0.028	0.773	0.189	0.011	0	0	0	0	0
15	0.015	0.730	0.242	0.013	0	0	0	0	0
16	0.008	0.702	0.271	0.018	0.001	0	0	0	0
17	0.005	0.651	0.320	0.024	0.001	0	0	0	0
18	0.002	0.611	0.356	0.029	0.001	0	0	0	0
19	0.001	0.556	0.406	0.035	0.002	0	0	0	0
20	0	0.500	0.451	0.046	0.003	0	0	0	0

**Probabilities obtained using Monte-Carlo simulation with 10,000 repetitions. Probabilities are rounded to the nearest 0.001. Probabilities of less than 0.0005 are rounded to 0.*

Table 1 provides the results of the Monte-Carlo simulation using parameters that are similar to those used in the experiments described in Section 3. The spatial extent of the target was ±2° (Φ = 2°). The clusters are assumed to be uniformly distributed within ±10° of **d**, therefore Ω=10°. In the simulations, the positions of M clusters were randomly drawn from a uniform distribution within ±Ω° (horizontally and vertically) and M_{in} was determined as the maximum number of overlapping clusters (clusters within a small window of ±Φ) anywhere in a range of ±Ω. For each M, the simulation was repeated 10,000 times, and the probability of having M_{in} 'inlier' clusters out of M is summarized in Table 1.

The results in Table 1 suggest that under the assumption that the subjects do not look at the targets (i.e., the clusters are uniformly distributed over the range ±Ω) it is very unlikely (probability of < 0.01) to have 5 or more 'inlier' clusters (that correspond to inlier samples selected by the Algorithm 1). For example, even for a large number of clusters, M = 20, the probability of having more than 4 inlier clusters is less than 1%. In the experiments described in Section 3, nine targets were presented for 2 seconds each. Assuming that on average two clusters are created for each target, there are 18 clusters in total (M = 18). According to Table 1, the probability of having M_{in} > 4 when subject's fixations are not correlated with the visual stimuli is less than 0.1%. The minimum percentage of inlier samples in the experiments reported in Section 3 was 26%, which under the assumption of clusters with equal durations, corresponds to 5 clusters. Therefore, according to Table 1, there is 99.9% certainty that the estimated values of $\tilde{\alpha}$ and $\tilde{\beta}$ in these experiments do not result from random eye movements that were not correlated with the presented targets (but rather from intermittent fixation on the presented stimuli). Table 1 can serve as a useful indication for the level of confidence in the estimated values of $\tilde{\alpha}$ and $\tilde{\beta}$.

3 Experiments

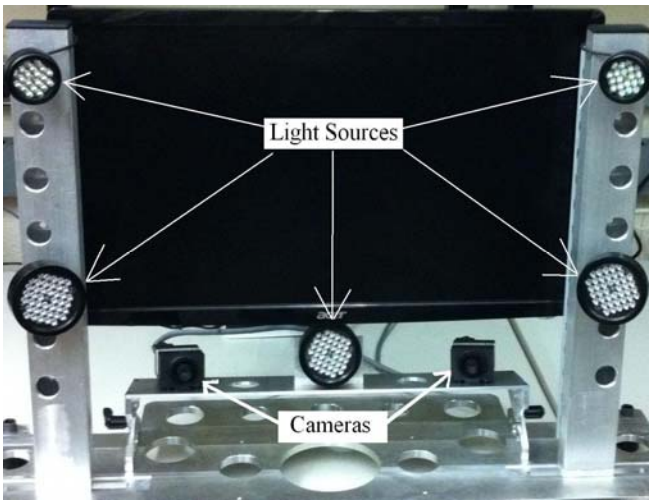

Figure 3. Prototype REGT system.

The experiments were carried out with the stereo-camera system shown in Figure 3. The study was carried out with 5 healthy infants (6, 8, 9, 15 and 16 months old). During the experiments, infants were seated on their parents' lap, with their heads supported by the parents' hands. Infants' head was approximately 85 cm from the computer monitor.

Nine 2cm X 2cm animated images (that is equivalent to 1.35° x 1.35° of visual field at a distance of 85 cm) were presented sequentially at different positions on the monitor and 450 estimates were recorded at a rate of 30 estimates per second. The measurement was repeated twice, to assess repeatability [Bland and Altman 1986].

The average difference (± Standard Deviation, SD) between two independent measurements of α^L, α^R, β^L and β^R was 0.04 ± 0.31° and the 95% limits of agreement for repeated measurements were ±0.61° (see Figure 4).

To test the methodology relative to a known benchmark (fixation on a calibration target), we have performed a one-point calibration procedure with 22 adult subjects. The adults were instructed to look at *one* of the animated images that were used during the experiments with the infants and 50 estimates of the direction of the optical axis were obtained. The angles α^L, α^R, β^L and β^R were calculated as described in Algorithm 1. The procedure was repeated twice for each subject. The average difference (± Standard Deviation, SD) between two independent measurements of α^L, α^R, β^L and β^R in adults was 0.03 ± 0.44° and the 95% limits of agreement for repeated measurements were ±0.87° (note that the size of the calibration target is 1.35° x 1.35° and subjects can fixate anywhere within the target). The slightly better repeatability with infants can be explained by the fact that by using more calibration targets with infants, differences in fixation positions within targets between repeated trials were averaged over more targets (i.e., the standard deviation of the differences between repeated estimates was reduced) which improved slightly the repeatability of the estimation procedure.

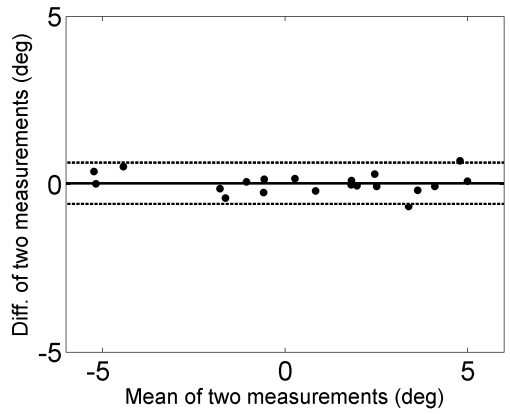

Figure 4. A difference vs. mean plot for two independent measurements of α^L, α^R, β^L and β^R (5 infants). The solid line indicates mean of differences (bias = 0.04°). The 95% limits of agreement (±0.61°) are indicated by the dashed lines.

4 Conclusions

An M-E procedure to estimate angle kappa in uncooperative subjects (infants) had been presented. M-E is based on a natural tendency of humans to look at patterned visual stimuli rather than at uniform fields. The M-E procedure does not require continuous fixation on calibration targets, however it does assume that there is a higher likelihood that the subject will fixate on the stimuli rather than anywhere else on the computer monitor.

In the experiments with 5 infants, the average percentage of time that infants looked at the stimuli was 47% (range from 26% to 70%). The average difference (± Standard Deviation, SD) between two independent measurements of α^L, α^R, β^L and β^R in infants was 0.04 ± 0.31°. The average difference (± Standard Deviation, SD) between two independent measurements of α^L, α^R, β^L and β^R in adults with one-point calibration procedure was 0.03 ± 0.44°. That is, the accuracy of M-E procedure is similar to the accuracy of one point calibration.

Even though the M-E procedure does not guarantee that angle Kappa can be estimated (i.e., when subjects do not look at the targets), the probability that the M-E procedure will provide a false estimate (an estimate that is associated with fixations that are *not* correlated with the calibration targets) can be assessed using the confidence measure derived in Section 2.3.

Acknowledgements

This work was supported in part by a grant from the Natural Sciences and Engineering Research Council of Canada (NSERC) and Canadian Institute of Health Research (CIHR) and in part by scholarships from NSERC and the Vision Science Research Program Award (Toronto Western Research Institute, University Health Network, Toronto, ON, Canada).

References

BLAND, J.M. and ALTMAN, D.G. 1986. Statistical methods for assessing agreement between two methods of clinical measurement. *The Lancet 327, 8476*, 307-310.

CARPENTER, R.H.S. 1977. *Movements of the eyes*. Pion, London, UK.

FANTZ, R.L., FAGAN, J.F. and MIRANDA, S.B. 1975. Early visual selectivity. In *Infant Perception: From Sensation to Cognition*, L.B. COHEN AND P. SALAPATEK Eds. Academic Press, New York, 249–345.

GUESTRIN, E.D. 2010. Remote, Non-Contact Gaze Estimation with Minimal Subject Cooperation. *PhD Thesis* Department of Electrical and Computer Engineering, University of Toronto, Toronto, ON, Canada.

GUESTRIN, E.D. and EIZEMNAN, M. 2007. Remote point-of-gaze estimation with free head movements requiring a single-point calibration. In *Proc. of Annual International Conference of the IEEE Engineering in Medicine and Biology Society*, 4556-4560.

GUESTRIN, E.D. and EIZENMAN, M. 2008. Remote point-of-gaze estimation requiring a single-point calibration for applications with infants. In *Proceedings of the Proc. of the 2008 Symposium on Eye Tracking Research & Applications*, Savannah, GA, USA, Mar. 2008 ACM, 267-274.

HASHEMI, H., KHABAZKHOOB, M., YAZDANI, K., MEHRAVARAN, S., JAFARZADEHPUR, E. and FOTOUHI, A. 2010. Distribution of Angle Kappa Measurements With Orbscan II in a Population-based Survey. *JOURNAL OF REFRACTIVE SURGERY 26, 12*, 966-971.

HELMHOLTZ, H. 1924. *Helmholtz's treatise on physiological optics. Translated from the 3rd German ed. Edited by J. P. C. Southall* Optical Society of America, Rochester, NY.

KOCH, C. and ULLMAN, S. 1985. Shifts in selective visual attention: towards the underlying neural circuitry. *Human neurobiology 4, 4*, 219-227.

MODEL, D. and EIZENMAN, M. 2010a. An Automatic Personal Calibration Procedure for Advanced Gaze Estimation Systems. *Biomedical Engineering, IEEE Transactions on 57, 5*, 1031-1039.

MODEL, D. and EIZENMAN, M. 2010b. User-calibration-free remote gaze estimation system. In *Proceedings of the 2010 Symposium on Eye-Tracking Research & Applications* ACM, Austin, TX, USA, 29-36.

NAGAMATSU, T., SUGANO, R., IWAMOTO, Y., KAMAHARA, J. and TANAKA, N. 2010. User-calibration-free gaze tracking with estimation of the horizontal angles between the visual and the optical axes of both eyes. In *Proceedings of the 2010 Symposium on Eye-Tracking Research & Applications* ACM, Austin, Texas, 251-254.

SCHAEFFEL, F. 2002. Kappa and Hirschberg Ratio Measured with an Automated Video Gaze Tracker. *Optometry & Vision Science 79, 5*, 329-334.

SHIH, S.-W., WU, Y.-T. and LIU, J. 2000. A calibration-free gaze tracking technique. In *In Proceedings of 15th Int. Conference on Pattern Recognition* 201-204.

SHIH, S.W. and LIU, J. 2004. A novel approach to 3-D gaze tracking using stereo cameras. *IEEE Transactions on Systems, Man, and Cybernetics, Part B: Cybernetics 34, 1*, 234-245.

YOUNG, L.R. and SHEENA, D. 1975. Survey of eye-movement recording methods. *Behavior Research Methods & Instrumentation 7, 5*, 397-429.